 FDMP, vol.10, no.2, pp.279-298, 2014

Numerical Study of Melting Coupled Natural Convection Around Localized Heat Sources

Mustapha Faraji[1], **El Alami Mustapha and Najam Mostafa**

Abstract: A study is reported of heat transfer and melting in a fan-less thermal management system consisting of an insulated horizontal cavity filled with a phase change material (PCM) and heated from below by a conducting plate supporting three identical protruding heat sources. Such a PCM enclosure can be used as a heat sink for the cooling of electronic components. The advantage of this cooling strategy is that PCMs characterized by high energy storage density and small transition temperature interval, are able to store a high amount of heat (thereby providing efficient passive cooling). A two-dimensional simulation model is developed that accounts for heat transfer by conduction, convection in the molten region and phase change. In particular, numerical investigations are conducted using an enthalpy-porosity method in order to examine the impact of the considered geometry on the temperature distribution and evolution in the enclosure. A wide range of values of the enclosure aspect ratio is considered.

Keywords: Phase change material, melting, enthalpy method, latent heat storage, electronic cooling, fan-less.

Nomenclature

A	aspect ratio, H_m/L_m
c_p	specific heat , J kg^{-1} K^{-1}
EC	electronic component
f	liquid fraction
h	enthalpy, J kg^{-1}
H_c	characteristic length, m
H_m	height of the enclosure, m
k	thermal conductivity, W m^{-1} K^{-1}

[1] Physics Department, LPMMAT Laboratory, Faculty of Sciences Ain Chock, Hassan II University, PO 5366- Maarif, Casablanca- Morocco. Corresponding author. Email: farajimustapha@yahoo.fr; Tel: +212 -631-756 -990

L_c length of the horizontal face of the component, m
L_e space between two consecutive heat sources (m)
L_m width of the enclosure, m
p pressure, Pa
Q' heat generation within heat source per unit length, W m^{-1}
S source term
t time, s
T temperature, K
u, v x , y velocity, m s^{-1}
X_c electronic component thickness , m
X_s substrate thickness , m

Subscripts

$1, 2, 3$ refer to the bottom, median and the upper electronic components, respectively.
c heat sources
cr critical value
l liquid, local
$m, l-m$ melt, PCM
max maximum value
p constant pressure
ref reference value
s wall, solid

Greek symbols

α thermal diffusivity (m^2 s^1)
β volumetric thermal expansion factor of PCM liquid (K^{-1})
$\delta_{1,2}$ Kronecker symbols
η distance perpendicular to the wall- heat sources/liquid PCM interface
ν Kinematic viscosity (m^2 s^{-1})
ρ density (kg/m^3)
ψ stream function, $\psi = (1/\alpha) \int udy - vdx$
ΔH_f latent heat (J kg^{-1}),
M dynamic viscosity (kg m s^{-1})

1 Introduction

The trend toward denser packaging and higher heat dissipation in compact small-size electronic devices has resulted in more attention to the analysis of the related thermal performances. Many modern devices (laptops and ipods) are slender and light [Tilley et al. (2001)].

The size and thickness of a variety of portable electronic devices are decreasing. By contrast, the power densities of the electronics, science instruments, and avionics in miniaturized devices are expected to exceed 300 W/cm^2 [Intel (2008)] in few years Due to the limited space available in such devices, this trend is making it difficult for engineers to find proper solutions for thermal management. Indeed, increased heat fluxes at all levels of packaging from chip to system to facility pose a major cooling challenge. To meet the challenge, significant cooling technology enhancements will be needed in each of the following areas [Garimella (2006)]: High thermal conductivity materials; Thermal interfaces; Heat spreading; Air cooling; Indirect and direct water cooling; Immersion cooling; Refrigeration cooling; Thermoelectric cooling; Equipment-facility interface; Transient Phase Change energy storage systems (PCM passive cooling); Passive two-phase devices such micro heat pipes embedded in electronic packages; Micro channel transport and Micro pumps; Jet impingement; Miniature flat heat pipes and Piezoelectric fans.

Several strategies can be used in principle to improve cooling efficiency.

There have been numerous studies on electronic cooling using various natural/ forced convection possibilities [Aung et al.(1972); Arid et al. (2012); Maougal et al. (2013)]. A combined numerical and experimental investigation was reported by Jaluria (2008) and Incropera (1999) who developed a design methodology for estimating electronic temperatures and choosing the optimum geometry. As an additional example, [Mahrouche et al. (2013)] investigated numerically mixed convection in a rectangular partitioned cavity equipped with two heated partitions at a constant temperature. The vertical walls were featured by openings. Their results show that the flow and heat transfer depend significantly on block height. Correlation for the dimensionless heat evacuated trough the opening was derived.

As an alternate strategy, materials with high thermal conductivity such as aluminum, copper and carbon fiber have been frequently used for thermal management of microelectronics and flat plate-type *heat pipes* have been particularly considered to overcome the limits in application that circular- and pressed type heat pipes have been undergoing. Although a heat pipe has a critical advantage of a high thermal conductivity, the actual thin versions developed for application in small package structures demonstrate a low thermal performance. This is due to an increase in flow resistance by a counter flow created between the vapor and liquid, as well as

to a difficulty in securing proper vapor flow space [Kirshberg (2000)].

An *active thermal solution* has a fan (either axial or blower type fan) directly mounted on heat sink as an unified heat removal device. System acoustic (from heat sink fan) and cost are the common trade-offs for an active heat sink [Incropera (1999); Tummala (2001); Shanmugasundaram et al. (1997)].

Passive thermal solution (fan-less) is a thermal solution without fan. The cost is obviously reduced [Intel (2008)]. In such a context, the use of phase change materials (PCMs) for passive cooling seems to be a promising alternative method of thermal management of periodically operating components (for various applications such as spacecraft thermal control, communication equipment and wearable laptops), due to relative high removal capabilities of PCMs compared with liquid and air options. The concept is simple as it uses specific cavities filled with PCMs as the heat sink. The use of PCM as a storage medium can reduce the size of the cooling system and allows a continuous cooling capacity.

During the working period, electronic components dissipate heat through their exposed faces and the solid PCM continually melts absorbing heat. The heat stored in the PCM is naturally rejected to the ambient as the melted PCM re-solidifies during the device stop periods [Faraji et al. (2010)].

To solve the problem of microprocessors overheating a hybrid heat sink combining fins and PCM reservoir was suggested by Wang et al. (2007). In the experimental author's results, the PCM thermal storage unit (TSU) showed that PCM reservoir will effectively keep high power density electronic components below their upper temperature limit. Another experimental study of melting and natural convection in an enclosure with three discrete flush heat sources attached on one of its vertical adiabatic wall was conducted by Binet et al. (2000). Results show that the rise in the temperature of heat sources can be reduced to 50 % by using PCM.

It should be noted that modeling of phase-change processes presents a significant challenge, due to complexity and interplay of the involved physical phenomena. Various approaches were attempted to overcome these difficulties. Pal et al. (2001) studied computationally and experimentally the melting of a PCM in a side uniformly heated (isothermal wall) tall enclosure of aspect ratio 10 for avionics applications. Ju et al. (1998) experimentally studied the melting process of n-octadecane in a rectangular cavity with three discrete protruding heat sources, placed on the vertical side of the enclosure. Cooling management of CPU was also investigated by Faraji et al. (2008) using a hybrid heat sink consisting of rectangular cavity filled with PCM attached to the conventional aluminum fins with a density of heat flux imposed to the base of the microprocessor. Krishnan et al. (2005) analyzed a hybrid plate fin heat sink with the tip immersed in a phase change material. The

influence of the location, amount, and type of PCM, as well as the fin thickness on the thermal performance of the heat sink was considered. It was found that the fin heat transfer rate increased with an increase in fin thickness and amount of PCM.

Inaba et al. (2003) and O'Connor et al. (1997) presented an extensive list of references on PCM- based heat sinks reported in the literature. The present paper is concerned with the modeling and numerical simulation of the melting process and natural convection within an isolated horizontal cavity filled with PCM and heated from below by a printed circuit board (on which protruding heat generating electronic components with a constant and uniform volumetric heat generation are mounted).

The objective of the present study is to explore the thermal behavior of a PCM based heat sink and examine the effects of the PCM cavity aspect ratio on the maximum temperature. Thermal and velocity fields within PCM cavity and the temperature profile in the substrate are also presented and analyzed.

2 Mathematical modeling

2.1 The Physical model

Figure 1 presents the physical model. It consists of a horizontal rectangular enclosure containing a PCM heated by three identical electronic components ($EC_{1,2,3}$) attached to the bottom wall.

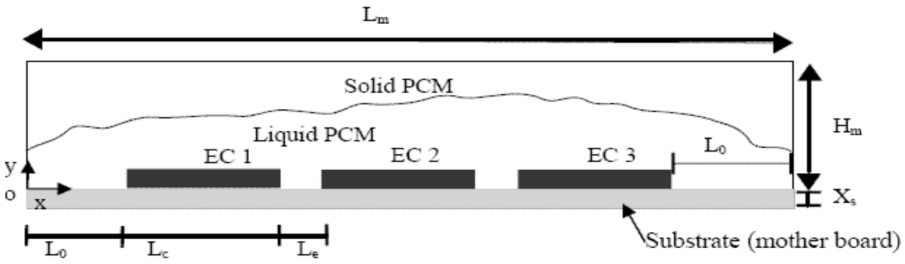

Figure 1: The physical model.

In most recent computer assembly mother boards, there are three electronic components directly related to the generation of heat: microprocessor, on-board graphical controller and chipset. These components contribute to the greater portion of the amount of the total heat generated within the computers. In addition, a wide range of computers are laptops. Furthermore, the modern laptops are slender. These are the reasons and motivations behind choosing the current configuration (three protruding electronic components attached to a horizontal substrate and no fan).

The height and thickness of each heat source are L_c and X_c, respectively. The distance between two consecutive heat sources is, L_e, and the distance between the left enclosure wall and the first heat source is, L. The height and width of the enclosure are, H_m, and, L_m, respectively. The thickness of the plate (substrate mother board) is, X_s. Each electronic component generates heat at constant and uniform rate, Q', and dissipates that heat through their exposed faces to PCM. The enclosure boundaries are adiabatic. Substrate participates by spreading and diffusing the heat to the PCM. The velocity field is subjected to no-slip boundary conditions at the walls. The flow is assumed to be two-dimensional, Newtonian, laminar and incompressible. The physical properties of the materials are constant at the temperature range under study. The density difference between solid and liquid phases is negligible, and the Boussinesq approximation is used to express the linear temperature dependence of the liquid PCM density in the momentum equation for the vertical direction. The phase change is isotherm and the PCM is assumed initially solid at temperature equals to its melting temperature, $T_o = T_m$.

2.2 Governing equations

The general form of the equation governing heat and mass transfer and flow in the studied configuration is as follows:

$$\frac{\partial(\rho\Phi)}{\partial t}+\frac{\partial(\rho u\Phi)}{\partial x}+\frac{\partial(\rho v\Phi)}{\partial y}=\frac{\partial^2(\Gamma\Phi)}{\partial x^2}+\frac{\partial^2(\Gamma\Phi)}{\partial y^2}+S_\Phi \tag{1}$$

Terms of the above equation are summarized in the Table 1.

Table 1: Terms of the general equation.

Φ	Γ	S_Φ
1	0	0
U	μ	$-\frac{\partial p}{\partial x}+S_u$
V	μ	$-\frac{\partial p}{\partial y}+S_v$
H	k/c_p	S_T

here,

$$\begin{cases} h = \int_{T_m}^{T} c_p dT + \mathrm{h(T_m)} \\ \mathrm{S_u} = -\mathrm{C}\dfrac{(1-\mathrm{f})^2}{(\mathrm{f^3}+\mathrm{b})}\mathrm{u} \\ S_v = -C\dfrac{(1-f)^2}{(f^3+b)}v + \rho_{ref} g\beta(T-T_m) \\ S_T = \delta_1\left(-(1-\delta_2)\rho\Delta\mathrm{H}_f\dfrac{\partial f}{\partial t} + \delta_2\dfrac{Q'}{X_c.L_c}\right) \end{cases} \tag{2}$$

S_u and S_v are source terms used for the velocity suppression in the solid regions (solid PCM, substrate and heat sources). One of the common models for the velocity suppression is to introduce a Darcy-like term [Voller et al. (1987), Lappa (2002)] (C=10^{25} kg m^{-3}s^{-1} and b= 0.005 are used). The same full set of governing equations throughout the entire enclosure governs conjugate heat transfer in both the liquid and solid regions with taking a large value of the viscosity in solid regions. The conductivity$k$and the step function δ are set as follows:

$$\begin{aligned} \delta_1 &= \begin{cases} 1 & \text{forelectroniccomponentsandPCM} \\ 0 & \text{forthesubstrate} \end{cases} \\ \delta_2 &= \begin{cases} 1 & \text{forelectroniccomponents} \\ 0 & \text{forthePCM} \end{cases} \\ k &= \begin{cases} k_m & \text{forPCM} \\ k_s & \text{forsubstrate} \\ k_c & \text{forelectroniccomponents} \end{cases} \end{aligned} \tag{3}$$

where the PCM thermal conductivity k_m and different physical properties of materials are expressed as follows:

$$\begin{aligned} &k_m = fk_{m,l} + (1-f)k_{m,s}, \quad (\rho c_p)_m = f(\rho c_p)_{m,l} + (1-f)(\rho c_p)_{m,s}, \\ &\alpha_m = f\alpha_{m,l} + (1-f)\alpha_{m,s}, \quad \mathrm{k_i} = \frac{\mathrm{k_+ k_-(\delta_+ + \delta_-)}}{\mathrm{k_+\delta_- + k_-\delta_+}} \end{aligned} \tag{4}$$

δ_+ and δ_- are distances separating the interface to the first neighboring nodes, '+' and '-'. k_+ and $k_-$are the thermal conductivities at nodes '+' and '-', respectively.

2.3 Boundary conditions

At the interfaces between two different materials (1) and (2) (substrate, PCM or heat sources):

$$k_1 \left.\frac{\partial T}{\partial \eta}\right|_{interface} = k_2 \left.\frac{\partial T}{\partial \eta}\right|_{interface}, \quad T_1 = T_2(\eta \perp \text{interface}) \tag{5}$$

At the adiabatic walls:

$$\left.\frac{\partial T}{\partial \eta}\right|_{wall} = 0 \tag{6}$$

No slip and non permeability at the solid interfaces and walls:

$$u = v = 0 \tag{7}$$

2.4 Initial conditions

$$u = v = f = 0, \quad T = T_m \tag{8}$$

The governing equations are discretized in a staggered mesh, with 180 nodes in the (ox) direction and 60 nodes in the (oy) direction, using a finite volume method developed by Patankar (1980). The power law scheme is used to evaluate the total flux which combines convective and conductive terms. The SIMPLE routine is used to couple pressure and velocity equations [Patankar (1980)]. It should be noted that the energy equation for the PCM is formulated using the enthalpy fixed-grid technique [Voller et al. (1987)]. The central feature of this technique is the source term S_T which keeps track of latent heat evolution, and its driving element is the local liquid fraction f. This fraction takes the values of 1 in fully liquid regions, 0, in fully solid regions, and lies in the interval]0,1[in the vicinity of the melting front. Its value is determined iteratively from the solution of the enthalpy equation as:

$$\begin{cases} f = 1 & \text{if} \quad T > T_m \\ f = 0 & \text{if} \quad T < T_m \\ 0 < f < 1 & \text{if} \quad T = T_m \end{cases} \tag{9}$$

The resulting algebraic equations are solved, for every time step, using the Tri-Diagonal Matrix iterative method. The model was implemented by developing a personal computer code in C language. Typical execution times for the fine mesh runs exceed 3 hours in a (CPU 3 GHz, 2 Gb RAM) desk computer. In order to estimate the convective heat transfer to the liquid PCM from each heat source,

average heat sources Nusselt numbers, based on the maximal temperature T_{max} , were calculated as follows:

$$\mathrm{Nu}_{1,2,3} = -\frac{1}{(L_c + 2X_c)\ (\mathrm{T}_{\max} - T_f)} \int_0^{L_c+2X_c} \mathrm{k_i} \left.\frac{\partial \mathrm{T}}{\partial \eta}\right|_{\mathrm{i}} \mathrm{d}\xi \tag{10}$$

where $d\xi$ design the heat source peripheral element length.

2.5 Validation

The computer program was used for validation against experimental data obtained by Ju et al. (1998) for a particular configuration of protruding heat sources similar to the present system. But the heat sources are mounted on a vertical wall. This configuration consists of an insulated rectangular enclosure of height, H_m = 9.0 cm, and width, L_m = 6.0 cm. The left vertical wall is made with Plexiglas material and have a thickness of, X_s = 2 cm. It supports three protruding heat sources of height, L_c = 1.5 cm, and thickness, X_c = 0.9 cm. The heat flux density delivered by each heat source equals to 900 W/m^2. The lower heat source is placed at a distance L= 0.75 cm to the bottom wall and the distance between two consecutive heat sources equals to L_e = 1.5 cm. Initially, the cavity is filled with a solid PCM (n-octadecane) at its melting temperature, T_m = 28°C. An air layer of 1 cm thickness was provided for PCM expansion during the melting. The numerical code was adjusted to meet setup conditions and, after a grid refinement (aspect ratio A = 1.5), the computer program results are compared with experimental results. It can be seen, taking into account the complexity of the phenomenon, that there is a satisfactory agreement between the present and published experimental data, as shown in Figure 2. The concordance is better at t = 25 min and t = 50 min except at the lower and upper heat sources that seem to be furnishing less heat to the PCM in comparison with the predictions of what predicts the mathematical model. Other reasons are also behind this slightly difference in melting front positions: the surrounding heat lost and due to the removal of the insulation during photography of the melting front. At t = 95 min and t = 110 min, the agreement is good, but a deviation at the top portion was clearly observed. Indeed, an amount of melted n-octadecane expands during the melting process and the hot liquid exits over and goes up the free surface of solid PCM and accelerates its melting. This explains the deviation to the right of the experimental melting front. A part of the liquid PCM comes out of the computational domain and breaks the adiabatic condition in the north boundary.

3 Results and discussion

Numerical investigations were initially conducted using a base case (Tables 2 and 3). These values frequently used in electronic industry. Initially PCM (n- eicosane)

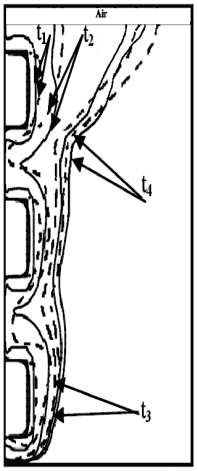

Figure 2: A comparison between numerical predicted melting fronts (solid lines) and photographed melting fronts obtained by Ju et al. (1998) (dashed lines) at t_1= 25 min, t_2= 50 min, t_3= 95 min and t_4= 110 min.

is in solid state ($T_o = T_f$= 36 ˚C). The studied heat sources represent the 4^{th} generation of microprocessors (CPU double Core Duo, used in recent laptops [5]). The main objective of the present study is to eliminate as possible the fan. The heat generated within microprocessors should be stored and absorbed in PCM reservoir. When the user switch on the laptop, CPU temperature rises and reaches, after a secured working time, the limiting temperature, $T_{cr} \sim 75$˚C, since it is typically the highest operating temperature permissible for most chips to ensure reliability. The time t_{cr} required by the electronic components to reach this limit temperature depends on the geometric and operating parameters of the cooling system. In view of this, numerical simulations were conducted during the limiting time t_{cr} or until the liquid fraction $f$approaches 1. In this study, the effects of the aspect ratio, A, is examined

PCM mass is represented by the quantity ($H_c^2 = H_m L_m - 3X_c L_c$) and was determined to ensure about two hours of secured working time without energizing the fan and. This duration is calculated assuming that all the power generated within heat sources (with Q'= 30 W/m) is completely absorbed by PCM and used to melt the PCM (there is no sensible heat storage). The duration can be estimated as follows:

$$t_{min} = \frac{\rho_m \Delta H_f H_c^2}{3Q'} \tag{11}$$

Therefore, using eq. (11) , the characteristics length, $H_c = \sqrt{L_m H_m - 3 X_c L_c}$=006m. it should be noted that when varying the aspect ratio, A quantity, H_c,is kept constant, hereafter cavity dimensions, H_m, and, L_m, are dependent variables and must be calculated for each value of the aspect ratio, A, using the following equation:

$$H_m = \sqrt{A\left(1+3\left(\frac{X_c L_c}{H_c}\right)^2\right)}\ ,\ L_m = \sqrt{\frac{\left(1+3\left(\frac{X_c L_c}{H_c}\right)^2\right)}{A}} \tag{12}$$

Table 2: Physical properties [Incropera (1999); Intel (2008); Tummala (2001); Humphries et al. (1977)].

Electronic component (alumina ceramics)	$\rho_c = 3260$ kg/m^3 $c_{p,c} = 740$ J/kg K k_c = 170 W/m K T_{cr} = 70 °C
Conducting Plate (Al substrate)	$\rho_s = 3900$ kg/m^3 $c_{p,s} = 900$ J/kg K k_s = 19.7 W/m K
PCM (n-eicosane)	β = 8.5x10^{-4}K^{-1} $\Delta H_f = 2.47$x10^{5}J/kg T_f = 36 °C $c_{p,m} = 2460$ J/kg K k_m = 0.1505 W/m K $\rho_m = 769$ kg/m^3 $\mu_m = 4.15$x10^{-3}kg/m s

Table 3: Base case geometrical dimensions (m).

X_c	L_c	L_e	X_s
0.003	0,015	0.010	0,005

3.1 Analysis of the base case.

Figure 3 shows the time wise evolution of maximal and averages electronic component temperatures. Also mean PCM temperature and liquid fraction are presented.

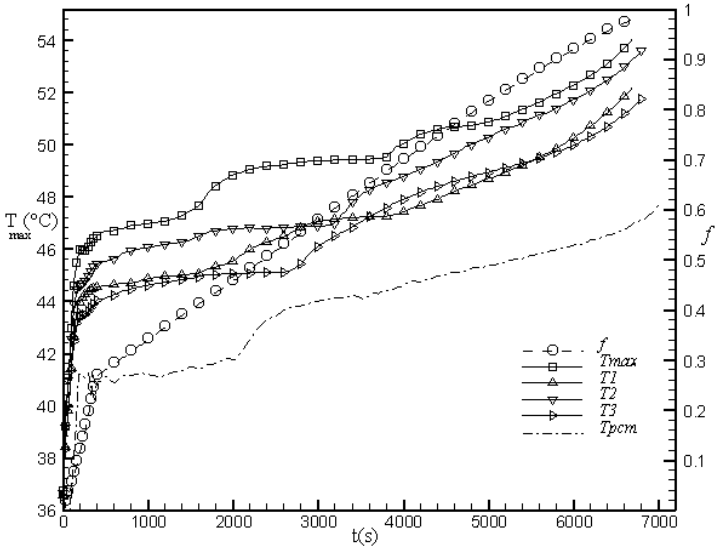

Figure 3: Temporal evolution of the electronic components maximal temperature, average PCM and heat sources temperature, PCM temperature and liquid fraction.

The melting process develops throughout three stages: pre melting, melting and post melting. During the first stage ($0 < t < 400$ s), heat sources temperatures are almost identical and increase rapidly and linearly. The power generated within each heat source is stored within it-selves and conductive heat transfer mode prevails in the slender liquid layer located at the vicinity of the electronics and conducting plate hot surfaces. Isotherms remains parallel to the bottom hot wall (Figure 4, t = 100 s). Indeed, Figure 5 shows that heat source average Nusselt number, *Nu,* decreases rapidly during the first stage due to the increase in thickness of that immobilized liquid layer. Thermal field stratifies in the molten region (hot liquid under cold liquid layers) and this unstable equilibrium will be broken after about t = 400 s and liquid motion starts. Rayleigh-Bénarde convective cells take place over the hot walls and isotherms are obviously distorted because of developing wall jets (panache structures, Figure 4, t= 1200 s). The onset of natural convection aids electronic components to reject their heat. In fact, liquid PCM strikes hot electronics components and becomes hotter. The lightning liquid flays in the ascending direction, erodes the melting front, loses it heat and the liquid becomes heavier. The cold liquid turns down and travels towards heat sources to cool them naturally. Liquid cavity grows and during the second stage, heat generated within heat sources is absorbed by the melting front (latent heat of fusion storage) and there is no sensible heat stored in liquid PCM or in electronic components. Therefore heat sources and

PCM temperatures remain practically constant (the plateau region in curves Figure 3).

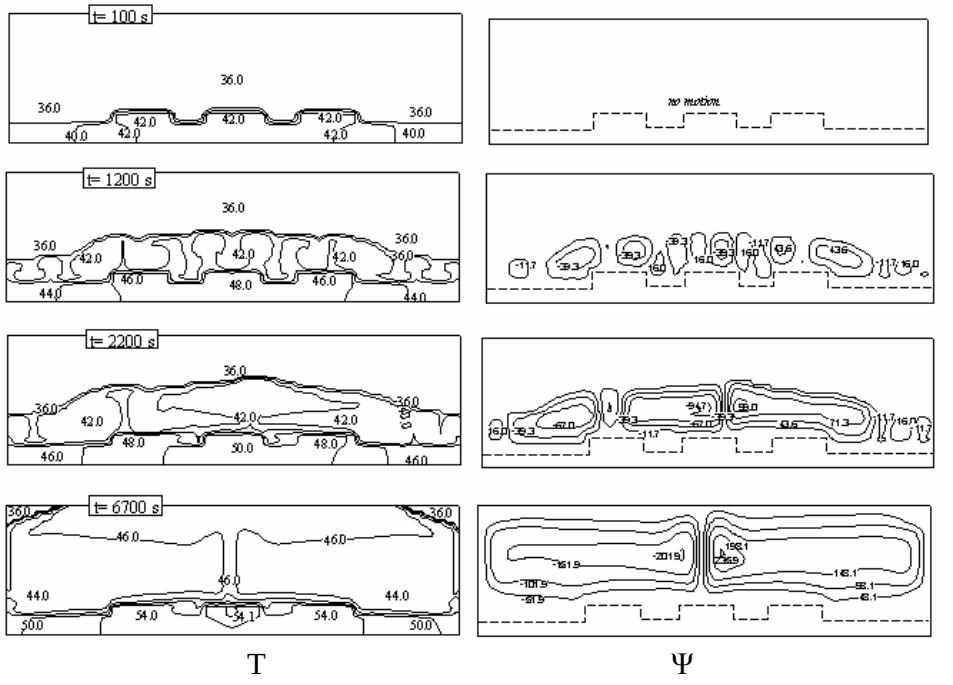

Figure 4: Temporal evolution of the thermal field (isotherms, T) and dynamic field (streamlines, Ψ).

This result can be confirmed when analyzing Figure 5 giving heat source Nusselt number, *Nu*. During the plateau region, Nussel number, *Nu* remains constant showing that the power generated from heat sources is completely absorbed by solid PCM and, as a result electronic component temperature remains practically constant and the system reaches quasi steady state regime, (400 s$< t <$ 2000 s). During the quasi steady state regime, convective cells locate above the hot wall. Convective flow strengthens and remains multicellular, but the cell's number decreases with time. Rayleigh-bénarde cells are, alternatively, clockwise and negative rotating vortexes. This behavior leads to the development of wall jet(isotherms, Figure 4, $t >$ 1200 s). The completion stage (rise of chip temperatures) begins when about 50% of the solid PCM is melted. The flow becomes bicellular and two opposite cells persist above heat sources. Natural convection intensify due to the increase in driven temperature between hot and cold walls (ΔT= 13˚C, ψ= 99 at$t$ = 2200 s and

ΔT= 18 °C, ψ= 2369 at t = 6700 s). Liquid temperature rises because of the enlargement of the liquid cavity and the distance between the hot wall and the melting front position (cold moving wall) increases and due to the lower value of PCM thermal conductivity, k_m =0.1505, sensible heat storage reactivates in the liquid cavity leading to an increase in PCM temperature, t >2000s. Therefore thermal gradients between heat sources and liquid PCM decrease, In fact, Nusselt number decreases (Figure 5) and, as a result, heat source becomes hotter as shown Figure 3,$t > 2000$ s. The melting process must sops when solid PCM is completely melted, $f \sim 1$, or when maximal temperature is near the threshold temperature, $T_{max} \sim T_{cr}$.

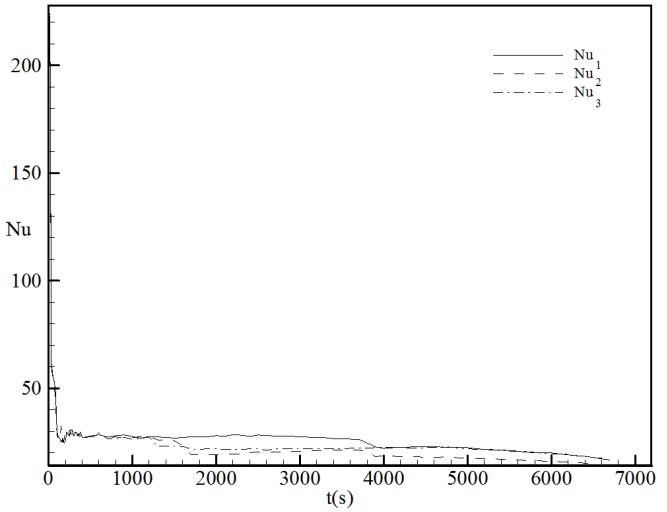

Figure 5: Temporal evolution of the electronic components average Nusselt numbers.

Heat generated by the modules has two distinct paths. It reaches the surface by conduction and convects away by the melted PCM stream or it spreads in the PC board (the plate). Since the plate and modules thermal conductivity ratios, $k_s/k_{m,l}$ and $k_c/k_{m,l}$ equal 130 and 1130 respectively, conjugate heat conduction coupled to the natural convection and solid/ liquid phase change are included in the present heat transfer model. The particularity of the present cooling strategy is that there is no fan, and the device works safely until the complete melting of the PCM or if one electronic component reaches the critical temperature T_{cr}. The above results were cheeked by analyzing the percentage heat transferred from the plate and through the exposed faces of modules to the core flow during the steady state regime. Table 4 summarizes the percentages of the mean heat flux transferred from various plate and electronic components exposed faces. Conducting plate (substrate) plays

the role of an interface capable to diffusing, spreading and conducting heat from heat sources to PCM cavity. Data analysis leads to conclude that the plate portions between modules transfer less heat to the core flow in comparison with the amount of heat delivered by the most side plate portions, because the trapped fluid remains pseudo stagnating in the micro cavity, (space between two heat sources) and the heat transfer occurs, at priory, by conduction in these locations. The heat transferred from the left and right side plate portions is the highest because of the larger surface of heat exchange between PCM and substrate in these portions of the enclosure. As was observed early in Figure 4, the high thermal conductivity of the substrate, relative to that of the PCM, allows for thermal spreading to occur through the substrate and no less than 48.50 % of heat generated in modules is transferred through the back face of the modules to the plate and convected to liquid PCM via the exposed plate faces (Table 3). The percentage of the generated heat which enters to the fluid through the modules exposed faces is around 48.00 %. It can also be deduced that the total heat absorbed by the PCM is found more than 96.00 %. Consequently, the cooling strategy based on PCM reservoir permits to absorb a high amount of the electronic components generated power without energizing the fan, and the device works safely, during about 7000 s until the complete melting of the PCM or if one electronic component reaches the critical temperature, T_{cr}

Table 4: Plate and modules heat transfer contributions (% heat generated in modules transferred to the PCM).

	14.40%		17,50%		16.10%	
17.40%	EC_1	6.70%	EC_2	7.00%	EC_3	17.40%
Plate						

3.2 Effect of the enclosure aspect ratio, A.

In this study, PCM quantity is kept constant, its value is represented by the constant length H_c, $H_c = \sqrt{H_m L_m - 3 L_c X_c}$. In order to keep constant the quantity H_c, when varying the cavity aspect ratio A, the cavity height, H_m and width, L_m, must be adjusted using the above relationship (Eq 12). Numerical simulations are driven with varying the aspect ratio within the range: A=1/16 to A= 1/4. Figure 6 shows the effect of the aspect ratio, A, on the time wise variation of the maximal temperature during the melting process. Temperature variations go to three regions: In the first stage, pure conduction prevails, and the corresponding temperature variations are nearly linear with time. Maximal temperature remains independent to the

aspect ratio until the onset of natural convection. During the second stage, natural convection develops, and all heat dissipated by the chips is transferred to the melting front and maximal chip temperatures rest practically constant and reach a temporary plateau region. It can be observed that electronic components temperature depends obviously to the aspect ratio during the quasi steady state regime. Indeed, for 600 s $< t <$ 1500 s, T_{max}= 45 ˚C A= 1/12 and T_{max}= 47 ˚C, A= 1/4. In the completion stage of the melting process, the temperature change is higher than that in the second region. For engineering view point, the aspect ratio A=1/8 gives the best solution (lower temperatures during about 7000 s). When analyzing the liquid fraction curves (Figure 6) we can distinguish two regions: conduction regime, $t <$ 500 s, and melting natural convection regime, $t >$ 500 s. During the conducting regime, liquid fraction increases rapidly and independently to the aspect ratio, because of thermal field stratification (before the onset natural convection). When natural convection develops, heat sources rejects easily there energy and heat spread rigorously in liquid cavity. The aspect ratio influences sensibly the liquid fraction variation.

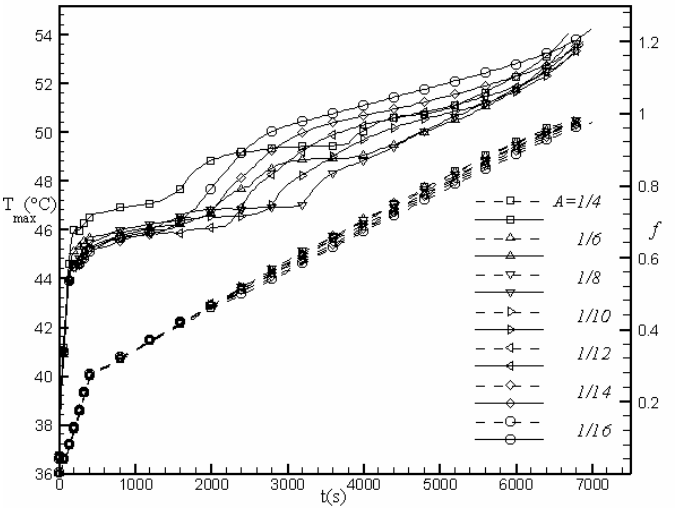

Figure 6: Temporal evolution of the electronic components maximal temperature, (solid lines) and liquid fraction (dashed lines); for various enclosure aspect ratio, A.

The same trends are revealed when Analyzing Figure 7 shows that. Indeed, during the quasi state regime, enclosure aspect ratio, A, has a substantial effect on the temperature profile in the conducting plate. When decreasing the aspect ratio, A, Heat transfer through the exposed plate portions is enhanced, which leads to a

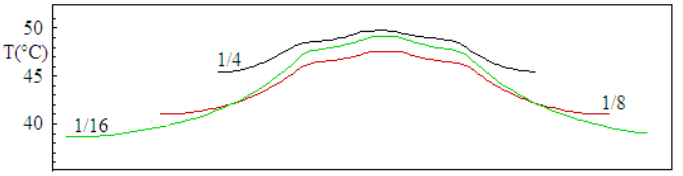

Figure 7: Substrate temperature profile dependency on the cavity aspect ratio A, $y = X_s/2$.

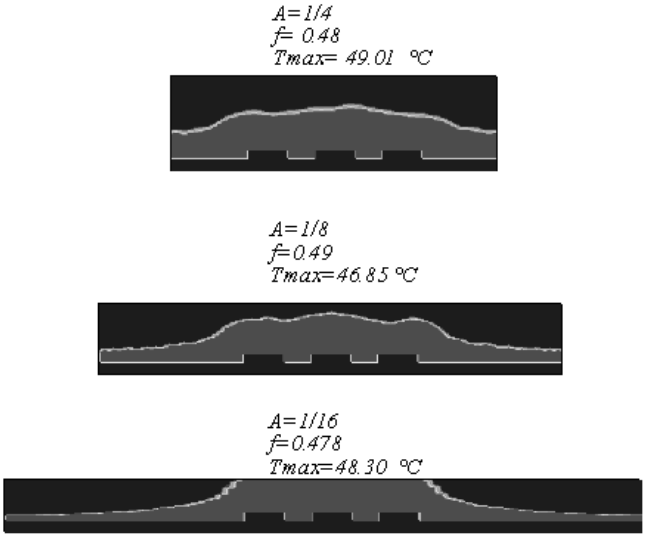

Figure 8: Melting front positions for different aspect ratios, A and, t= 2200 s.

reduction of electronic components temperature. But, it can be seen that more decreasing of, A, leads unfortunately to an unwanted negative effect: increase in the overall temperature difference in the substrate, $\Delta T_{s,\max}$, which is equal to $\Delta T_{s,\max}$= 4 ˚C for A= 1/4 and increases to 10 ˚C for A= 1/12. This relatively high thermal gradient found in the relatively thin plate (X_s =3 mm) for the aspect ratios $A <$ 1/12, can provoke a PC board serious split (crack). Also, we conclude that the use of isothermal or isoflux simple boundary conditions at the plate does not represent properly the heat transfer characteristics in the present situation.

The PCM solid–liquid interface shape and position, for different aspect ratios, A, are depicted in Figure 8. Analysis of such figure shows that, for A=1/4, because of the higher thermal diffusivity, and lower surface of the left and right sides portions of the plate, the melt sprawls rigorously along the bottom hot wall, appearing a

situation pseudo similar to the melting inside an isothermal wall and the melting front progress rapidly in these locations. With decreasing the aspect ratio, A, the sides conducting plate portions enlarges (because PCM mass was kept uncharged). Generated heat encounters more resistance to enter profoundly in the conducting plate and to the core PCM cavity side regions. This explains the shape of the melt front and the presence of the melt pockets surrounding locally the chips. It should be noticed that for lower aspect ratios, $A < 12$, solid PCM melts totally and rapidly above heat sources and an important quantity of PCM remains, unfortunately, none melted above the substrate.

4 Conclusion

Melting of a phase change material (PCM) in a horizontal rectangular cavity heated from below with three electronic chips mounted on a horizontal PC- board has been investigated numerically. It has been found that, phase change materials can be used to absorb transient power produced by powered electronics (used in laptops). Its use can also reduce the size of the cooling system (saving money, space, or other system resources). Numerical simulations were carried out to study the effect of the enclosure aspect ratio on the thermal performance of the cooling PCM based heat sink. It has been concluded that electronic components maximal temperature and melt fraction depend on the cavity aspect ratio. The results showed clearly that the PC- board temperature profile depends on the cavity aspect ratio thereby making irrelevant past studies where the effect of the aspect ratio was neglected. The duration of the plateau region, corresponding to the stable values of the chip's temperatures depends also on the cavity aspect ratio. Very important variations in temperature gradient were found in PC- board layer near electronic junctions for slender PCM cavities; this can create a serious split (crack) problem.

References

Arid, A.; Kousksou, T.; Jegadheeswaran, S.; Jamil, A.; Zeraouli, Y. (2012): Numerical Simulation of Ice Melting Near the Density Inversion Point under Periodic Thermal Boundary Conditions. *Fluid Dyn. Mater. Process,* vol. 8, no.3, pp. 257-276.

Aung, W.; Beitin, K. I.; Kessier, T. J. (1972): Natural Convection Cooling of Electronic Cabinets Containing Arrays of Vertical Circuit Cards, ASME Paper 72-WA/HT-40.

Binet, B.; Lacroix, M. (2000): Melting from heat sources flush mounted on a conducting vertical wall. *Int. J. Num. Methods for Heat and Fluid Flow,* vol. 10, no. 2, pp. 286 –307

Faraji, M. (2008): Numerical Optimization of a Thermal Performance of a Phase Change Material based Heat Sink. *International Journal of Heat and Technology,* vol. 26, no. 2, pp. 17-24.

Faraji, M. (2010): Numerical study of melting in an enclosure with discrete protruding heat sources. *Applied Mathematical Modelling,* vol. 34, pp. 1258–1275.

Garimella, S. V. (2006): Advances in micro scale thermal management technologies for microelectronics. *Microelectronics Journal,* vol. 37, pp. 1165–1185

Humphries, W. R.; Griggs, E. I. (1977): A Design Handbook for Phase Change Thermal Control and Energy Storage Devices. NASA Technical Paper 1074, NASA Scientific and Technical Information Office.

Inaba, H.; Matsuo, K.; Horibe, A. (2003): Numerical Simulation for Fin Effect of a Rectangular Latent Heat Storage Vessel Packed with Molten Salt under Heat Release Process. *Heat and Mass Transfer,* vol. 39, pp. 231–237.

Incropera, F. P. (1999): Liquid cooling of electronics devices by single phase convection, Wiley series in Thermal Management of Microelectronics and Electronics Systems, Wiley Inter Science Publications.

Intel - White Paper, June (2008): Nettop Platform for 2008 System Design

Jaluria, Y. (2008): Design and optimization of thermal systems. 2^{nd} ed. CRC Press Boca Raton London New York.

Ju, Y.; Chen, Z.; Zhou, Y. (1998): Experimental Study of melting heat transfer in an enclosure with three discrete protruding heat sources. *Exp. Heat Transfer,* vol. 11, pp. 171-186.

Kirshberg, J.; Yerkes, K.; Liepmann, D. (2000): Cooling Effect of a Mems-based Micro Capillary Pumped Loop for Chip-level Temperature Control. *ASME 2000, MEMS* vol. 2, pp. 143-150.

Krishnan, S.; Garimella, S. V.; Kang, S. S. (2005): A Novel Hybrid Heat Sink using Phase Change Materials for Transient Thermal Management of Electronics. *IEEE Transactions on Components and Packaging Technologies,* vol. 28, pp. 281-289.

Lappa, M.; Savino, R., (2002): A Novel 3D analysis of crystal/melt interface shape and Marangoni flow instability in solidifying liquid bridges. *Journal of Computational Physics,* vol. 180, pp. 751-774.

Mahrouche, O.; Najam, M.; El Alami, M.; Faraji, M. (2013): Mixed Convection Investigation in an Opened Partitioned Heated Cavity. *Fluid Dyn. Mater. Process,* vol. 9, no.3, pp. 235-250.

Maougal, A.; Bessaïh, R. (2013): Heat Transfer and Entropy Analysis for Mixed Convection in Discretely Heated Porous Square Cavity. *Fluid Dyn. Mater. Process,*

vol. 9, no.1, pp. 35-58.

O'Conner, J.; Weber, R. (1997): Thermal management of electronic packages using solid-to-liquid phase change techniques. *International Journal of Microcircuits and Electronic Packaging,* vol. 20, pp. 593–601.

Pal, D.; Joshi, Y. K. (2001): Melting in a side heated tall enclosure by a uniformly dissipating heat source. *International Journal of Heat and Mass Transfer,* vol. 44, pp. 375–387.

Patankar, S. V. (1980): Numerical Heat Transfer and Fluid Flow, Hemisphere, Washington, D.C,

Shanmugasundaram, V.; Brown, J. R.; Yerkes, K. L. (1997): Thermal management of high heat flux sources using phase change material, a design optimization, AIAA 97-245.

Tilley, A. R.; Associates, H. D. (2001): The Measure of Man and Women, Human Factors in Design, revised edition, Whitney Library of Design, Watson– Guptill Publications.

Tummala, R. R. (2001): Fundamentals of Micro systems Packaging, McGraw Hill.

Voller, V. R.; Cross, M., Markatos, N.C. (1987): An enthalpy method for convection/diffusion phase change , Int. J. for Num. Meth. Engng,; vol. 24, no. 1, pp. 271-284

Wang, X. Q.; Mujumdar, A. S.; Yap, C. (2007): Effect of Orientation for Phase Change Material (PCM)-based Heat Sinks for Transient Thermal Management of Electric Components. *International Communications in Heat and Mass Transfer,* vol. 34, pp. 801-808